Chapter 14

Generation and Evaporation of Microsprays

Chin-Tai Chen

Additional information is available at the end of the chapter

http://dx.doi.org/10.5772/64756

Abstract

This chapter aims to comprehensively review the techniques and features of micro-sprays for various applications via micro-droplet generators over decades, especially focusing on the past and present microfluidics. It is organized briefly as below. The background of current research and development about the micro-spray techniques is first introduced, followed by the generation and evaporation of spray detailed with the concentrated respects of critical requirements for materials and facilities. Then, we address the critical design issues of micro-sprayers such as the actuators and nozzles required to be satisfactory for generating a number of droplets. Subsequently, we further describe characterization of droplets in form of spray concerning droplet size, speed, rates, and patterns in microfluidics. Moreover, the chapter presents the proof-of-concept and commercial applications of the micro-spraying processes, highlighting their current technical progresses and future challenges, which shall be intimately related to the droplet generation and evaporation including droplet evaporative cooling, direct printing, screen printing, nanomaterial coating, liquid nebulization, and miscellaneous employment. Finally, we draw a conclusion in the end of the chapter.

Keywords: Spray, droplet generation, droplet evaporation, micro-actuator, microfluidics

1. Introduction

Over the past 30 years, spray droplets have been investigated and engineered due to their frequent occurrence in nature such as sea water [1] and manual generation on hot surfaces such as liquid deposition [2]. This field of science and engineering has widely demonstrated their significance on thermal and fluidic dynamics, in particular related to cooling and evaporation of spray droplets. Those numerous droplets, as being mechanically pumped through small nozzles of a continuous fluid delivery system, have been used for different respects of the evaporative cooling since then. Compared to the conventional mechanical droplet generators, another type of the modern microfluidic generators can eject the micron-

sized droplets through micro-electro-mechanical actuators that typically feature light weight, small size, less noise, and high power conservation [3]. Furthermore, as bonding with an array of micro-nozzles (orifices), a number of femto- to pico-liter droplets can be simultaneously generated at high driving frequency (kilo-to mega-Hz), forming a highly directional spray away from the nozzle surface [4].

To acquire high quality sprays in many applications (e.g., evaporative cooling), generating the droplets efficiently from certain micro-nozzles to a targeted space or surface exhibits technical requirements for key parameters [1], including the velocity of the droplets, the number flux of droplets, and the Sauter mean diameter. In terms of hydrodynamic properties, a stream of micro-droplets typically experience in either case below: (1) impacting, wetting, and evaporating (and depositing) on a two-dimensional (2D) surface and (2) floating and evaporating within a three-dimensional (3D) space. In both cases, the intrinsic non-uniformity of a spray generated from a single nozzle is frequently encountered in the conventional liquid delivery system, leading to the poor performance in some applications such as evaporative cooling. For example, non-uniform temperature distribution on the wall surface may be resulted from the different droplet-size distributions (DSDs) [5]. Likewise, it is possible to encounter a complex problem of determining the efficiency of evaporative cooling occurred with non-uniform distributions of droplets [6]. Moreover, non-uniform droplets forming turbulent flows can be also caused by ambient air and pressure within the zone of the spray, thereby significantly influencing the evaporation of spray droplets [7].

On the other hand, in the recent years, many efforts of research and development in academics as well as industries have been made to facilitate the various components and devices fabricated by the spray printing (SP) techniques, including amperometric enzyme electrodes [8], organic transistor electrodes [9], metal silver films [10], counter electrodes for flexible dye-sensitized solar cells [11], carbon thin films on flexible substrates [12], organic field-effect transistors and complementary inverters [13], flexible polymer solar cell modules [14], etc. Compared to the current inkjet-printing (IJP) techniques [15], this SP process is generally characterized with one additional screen (mesh) for patterning a variety of materials coated on substrate surfaces. Moreover, the screen printing by spray further provides a capability of large-area patterning on substrates without requirement of precise positioning, and therefore becomes an alternative low-cost technology consuming little material and power. Accordingly, using the SP techniques as a simple manufacturing tool, several global manufacturers have developed the material-processing equipment and peripheral utilities from the laboratory to commercial grade, for example, Legend Star International Co., Ltd. (http://www.lgs.com.tw) and Diamond-MT, Inc. (http://www.diamond-mt.com), in order to offer the customizing design services for academic research and commercial production.

In addition, with the remarkable emergence of nano-science and technology, many functional and novel materials have consequently been exploited to generate specific thin films and nanostructures using this SP method. For instance, a variety of fabrication methods for deposition of thin-film oxides (e.g., yttria-stabilized zirconia, YSZ) such as chemical vapor deposition (CVD), physical vapor deposition (PVD), electrochemical vapor deposition (EVD), spray pyrolysis, slip casting, screen printing, and so forth were comprehensively presented

and discussed by Will et al. [16]. Compared to the other methods, spray pyrolysis (of a metal salt solution) can be reliably utilized to form amorphous to polycrystalline microstructures (metal oxide films) at economical cost, although post-thermal treatment is usually necessary. Using this kind of spray techniques, the continuing efforts were made for the film production of copper and hybrid nanoparticles [17], the generation of metal particles [18], and the generation of metal and metal oxide nanoparticles [19]. Furthermore, more extensive studies for spraying applications were also directed to other advanced materials including biomedical calcium phosphate [20], colloidal dispersion of alumina particles [21], and composite materials of silver nanoparticles [22]. Importantly, many of the fundamental principles (e.g., preparation of pure liquid and solution materials) and utilities (e.g., setup of a liquid delivery and spray system) were commonly adopted in another nebulization application, for example, the aerosol and pulmonary drug delivery [23–25]. Therefore, full understanding of fundamental spraying mechanism here is a substantial effort to realize the key performances for such practical applications of the droplet generation techniques.

This book chapter concisely reviews the recent development of spray techniques and applications in our daily life and industry using micro-droplet generation, particularly benefiting the public in many respects such as saving energy, cost and time. It is organized briefly as follows. First, the background of the past and present development associated with the spray techniques is introduced here in Section 1, followed by the elaboration of the spray generation and evaporation regarding various liquids and actuators in Section 2. Section 3 presents the important design issues of micro-actuators/nozzles and integration/control, basically considering the implementation of spray. Section 4 describes the general characteristics of droplets existing in spray such as their sizes, speeds, volumetric rates, and fluidic patterns. Section 5 demonstrates the up-to-date applications of the micro-spraying processes, expressing the potential development and challenges in the future, which include droplet evaporative cooling (DEC), direct printing (DP) and screen printing (SP), nanomaterial coating (NMC), liquid nebulization (LN), and miscellaneous utilities. Finally, we draw a conclusion in Section 6.

2. Fundamentals of microspraying

Considering the common requirements of spray applications, a series of spraying processes should be comprehensively dealt with concerning the formation evolution of a spray: liquid supply and actuation, droplet generation, spraying, evaporating and deposition, as shown in Figure 1. Spraying droplets with different sizes (i.e., s_1, s_2,…, and s_n) may impact and wet on surface (i.e., d_1, d_2, and d_m) through evaporating (and $m < n$). As a matter of fact, every step here may involve technically serious considerations and significantly influence the performances of a spray-based system in the various applications. Those consideration factors in the successful spraying of materials and components are briefly described, discussed, and analyzed as below.

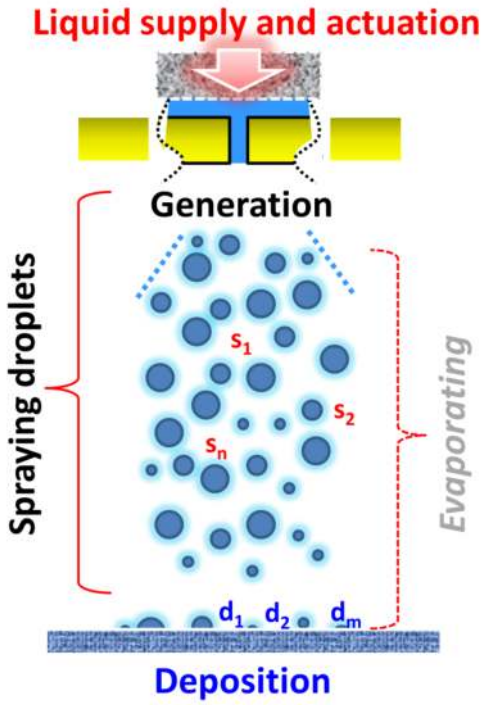

Figure 1. Schematic representation of spray generation and evaporation undergoing typically from one position of liquid supply and actuation (on the top) to another position of deposition on surface (at the bottom): those numerous droplets with various sizes are evaporating in air (s_1, s_2,…, and s_n) and on surface (d_1, d_2,…, and d_m).

2.1. Liquids and actuators

For many of applications, selecting suitable pure liquids or solutions is the most important factor in evaluating primary performances of spraying processes such as evaporative cooling efficiency and direct printing of materials. For pure liquids, their dynamic viscosities (e.g., pure water of 1.00 cp and ethanol of 1.09 cp at 20°C, where 1 cp = 1 mNs/m^2) should be low enough for the liquid delivery (through a tubing system) and ejection (from a powered actuator). Also, their surface energies in air are typically ranging from 20 to 73 mN/m in order to (e.g., pure water of 72.86 mN/m and ethanol of 22.39 mN/m at 20°C). For liquid mixtures, the solid contents (e.g., silver and gold nanoparticles) have to be effectively dispersed in the solvent (i.e., aqueous or non-aqueous) by additional suitable surfactant (e.g., detergents), in which particle aggregation is avoided for the long-term operation [26]. The particle sizes, in general ranging from a few to hundreds of nanometers (nm), are also small to a certain extent depending on some limits of the fluid delivery pipes and exit nozzles [10].

Second, the means of actuation powerfully pumping (dispensing) the liquid out of the nozzles should be considered for different needs. For instance, some mechanically pneumatic pumps

http://dx.doi.org/10.5772/64756

connecting to metal nozzles are able to eject high-throughput sprays robustly but noisily; therefore, they are most often exploited for evaporative cooling in large buildings and facilities [27–29]. However, at smaller scales, many new types of micro actuators such as piezoelectric [3–4,30] and electrostatic [14,31] ones are used to take advantage of precise electrical control over spray. Compared to the former (pneumatic), these microfluidic actuators may be further explored for versatile circumstances of daily life using novel and versatile materials.

Using the fluidic actuators filled with suitable liquids, a number of droplets can be therefore pumped from the small nozzles as electrically powered. In theory, those droplets generally exhibit spherical shapes in air due to intrinsic surface tension of liquid as demonstrated in Figure 1. Thus, the individual volume (V) and surface area (A) of a formed droplet are geometrically estimated in Eqs. (1) and (2):

$$V = \frac{4}{3}\pi \times R^3 = \frac{4}{3}\pi \times \left(\frac{D}{2}\right)^3 = \frac{\pi}{6} \times D^3 \tag{1}$$

$$A = 4\pi \times R^2 = 4\pi \times \left(\frac{D}{2}\right)^2 = \pi \times D^2 \tag{2}$$

where R is the radius and D is the diameter for a single drop, respectively. In general, the droplet size, volume, and surface area here rely on the size of nozzle. The conventional metal nozzles have quite diverse diameters ranging from tens of micrometers (μm) to a few millimeters (mm). By contrast, the micron-sized nozzles used in micro-actuators are generally found with 10–100 μm in diameter. As a result, those droplets are generated to exhibit the corresponding volumes with tens to thousands of pico-liters (pl = 10^{-12} l), primarily depending on the actuation means and devices. Obviously, the smaller droplets may be also yielded by simply reducing the nozzle diameter.

In fact, except for the called drop-on-demand (DOD) operation that is often used in IJP [32,33], the uniformity of size of individual droplets is one of the crucial factors considered for precise spraying in many applications [15]. For example, the thermal performances of a spray such as critical heat flux (CHF) can be significantly influenced by the deviation from the targeted value of the droplet size [34]. Hence, in many situations, it shall be substantially coped with the droplet size distribution as well as evaporation as follows.

2.2. Droplet size distribution and evaporation

The general droplet size distribution (DSD) in conventional sprays can be represented by classic Mugele-Evan (ME) relation as described in Eq. (3) [29,35], where $f_N(D)$ is the number (N) density distribution, and i and j are positive integers. Hence, the arithmetic mean diameter (AMD) (i.e., D_{10}, where $i = 1$, $j = 0$) is expressed in Eq. (4). Also, the well-known Sauter mean diameter (SMD) is defined for D_{32} (where $i = 3$, $j = 2$) as shown in Eq. (5) [36]:

$$D_{ij} = \left[\frac{\int_0^\infty D^i f_N(D) dD}{\int_0^\infty D^j f_N(D) dD} \right]^{\frac{1}{i-j}} \tag{3}$$

$$AMD = D_{10} = \int_0^1 D f_N(D) dD = \int_0^1 D dN \tag{4}$$

$$SMD = D_{32} = \frac{\int_0^\infty D^3 f_N(D) dD}{\int_0^\infty D^2 f_N(D) dD} = \frac{\int_0^\infty D^3 dN}{\int_0^\infty D^2 dN} \tag{5}$$

As the simplest case of a uniform spray, all of the droplets have the same diameter of D_s, thereby giving the AMD = D_{10} = D_s. Furthermore, in this special case, the SMD (i.e., D_{32}) can be clearly represented by the ratio of the single droplet volume (V)/surface area (A): D_{32} = 6×(V/A), according to previous Eqs. (1) and (2). Based on this concept of the ratio of V/A, the SMD shows particular significance in some circumstances, where the surface area plays a critical role such as droplet evaporation time in air, as shown in Eq. (6) [1]:

$$\tau = \beta \times \frac{\pi \times D_s^2}{\alpha(T)} = \frac{\beta \times A}{\alpha(T)} \tag{6}$$

where β is the dimensionless coefficient, D_s is the single droplet diameter, α is the thermal diffusivity of the droplet, and T is the temperature, respectively. For example, supposed that the water with the β = 3.23×10^{-2} and α = 1.43×10^{-7} m^2/s at 25 °C, a droplet of D_s = 100 μm is estimated with the evaporation time of τ = 7.10×10^{-3} s (i.e., 7.1 ms), while a shorter time of τ = 7.10×10^{-5} s (i.e., 71 μs) for a droplet with a 10-time smaller diameter (i.e., D_s = 10 μm).

2.3. Spraying control

In regard to the spraying control, it is mostly concerned with the volumetric rate of a spray. As can be seen in Figure 1, some of the droplets ejected out of nozzles (i.e., s_1, s_2, and s_n) might reach, deposit, and grow on certain surfaces (i.e., d_1, d_2, and d_m), even though they fulfill the evaporation (in air) as mentioned above. Therefore, real-time control over the spraying is another crucial part of the microfluidic actuation. For a pneumatic pumping/dispensing system, switching the actuation of a spray on and off is frequently completed in a period of a few seconds, in order to get rid of excessive growth of deposit.

To achieve high-speed switching, however, digital control over micro actuation can be carried out precisely for the new types of microfluidic actuators, where they can operate electronically at driving frequencies more than tens of kHz [30]. Utilizing the present computer-assisted capability over one decade, those control systems have been developed and implemented with

http://dx.doi.org/10.5772/64756

graphical user interface (GUI) by using commercial software such as MATLAB, LabVIEW, C, C++, and Visual Basic languages.

Based on the fundamental knowledge of spray science and technology, two preliminary design issues of micro-sprayers for realizing precise droplet generation are further addressed and discussed below.

3. Design issues of microsprayers

3.1. Micro-actuators and nozzles

As illustrated previously in Figure 1, the liquid supply and actuation forming a spray have to be performed at the first stage. For the purpose of effective formation of a spray as exemplified in Figure 2, the fluidic systems with different complexity can be designed and built here. Figure 2(a) shows an infrared (IR) thermography picture (NEC G100, JP) of a conventional pneumatic system (red) mainly composed of liquid supply (through tubing) and a metal nozzle (exit diameter of 80 μm, GAU PU GP-A008, TW). As being pressurized (70 kg/cm^2) from an electric pump (at 110 V, 850 rpm), droplet jetting of a water spray with a rate of 22 ml/min was continuously formed in a conical shape (see S). Meanwhile, it generated a loud noise of 85 dB from 50 dB (due to large mechanical vibration) and high humidity of 80 RH% from 60 RH% (due to excessive growth of deposit) in the neighboring space, substantially posing a notable disadvantage in some applications of the public daily life.

To avoid the induced noise and humidity, the actuators and nozzles can be largely miniaturized and arrayed for generation of a spray at the micron scale, as demonstrated in Figure 2(b). Here, the commercial ink cartridge installed in a bubble-type inkjet printer (Canon PIXMA iP 2770, JP) is composed of a print-head with a resolution of 1,200 × 4,200 dpi (1,472 fine nozzles, droplet volume of 2 pl). After de-capping the printer and removing the original ink from the cartridge, then pure water was manually re-filled from the liquid supply of a tubing container. By virtue of a microelectronic controller of the printer, the print-head was successfully actuated in scanning motion, so that water droplet jetting of 1 ml/min from its array of nozzles was achieved (see S). Compared to the previous one, a lower noise of 60 dB as well as humidity of 60 RH% was obtained in the same environment, indicating a great improvement in the spraying performance (i.e., decrease by 25 dB and 20 RH%) because of more uniform and fine droplets.

3.2. Microsystem integration and control

As using micro-actuators and nozzles, another design issue on the implementation of a microsprayer includes the microsystem integration and control required for many situations [3]. For example, as exemplified in Figure 3(a), an electrical power supply and a signal generator were equipped and controlled here to adaptively vary the driving voltage (v_{drive}, V) and frequency (f_{drive}, kHz) for a micro-actuator (e.g., piezoelectric actuation). Consequently, droplet ejection of a spray is able to be finely tuned for optimal performance [4,30]. The droplet

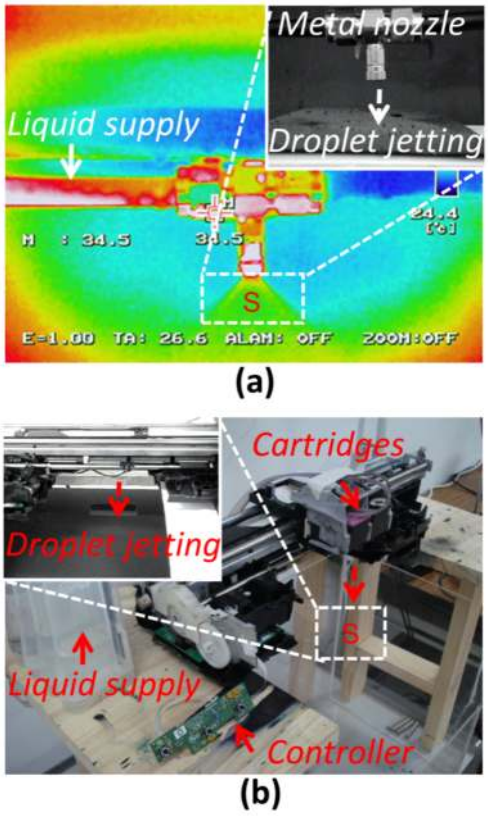

Figure 2. Demonstration and comparison with two types of spraying components and systems: (a) typical jetting process of water generated from liquid supply to a metal nozzle using a mechanical pump and (b) water droplets jetting from a liquid supply to a print-head cartridge with micro-actuators and nozzles using an inkjet printer.

velocity and volumetric rate for a spray may increase as raising the values of v_{drive} and f_{drive}. In addition, the compact liquid supply system comprising a tube and a container can be integrated and packaged with this microfluidic actuator (symbolized by A), as schematically depicted in Figure 3(b). Following the way, the fluid was expected to be slowly delivered (with an inner tubing diameter of 10 mm) from the bottom inlet to the top outlet (total vertical distance of 120 mm) as powered by microelectronic control and actuation (at v_{drive} and f_{drive}).

Such microsystem integration and control was realized by using a piezoelectric actuator under a suitable condition. As demonstrated in the IR thermography of Figure 3(c), one upward water spray was continuously generated in a period of 180 s from the fluidic outlet of the actuator (at v_{drive} of 60 V, f_{drive} of 90 kHz). However, their morphologic features changed apparently over time (i.e., 30, 90, and 180 s) implying the variation in physical properties (e.g., velocity and rate) and geometric pattern (e.g., turbulent flow). Hence, those characteristics of droplets within a spray are described and analyzed next in Section 4.

http://dx.doi.org/10.5772/64756

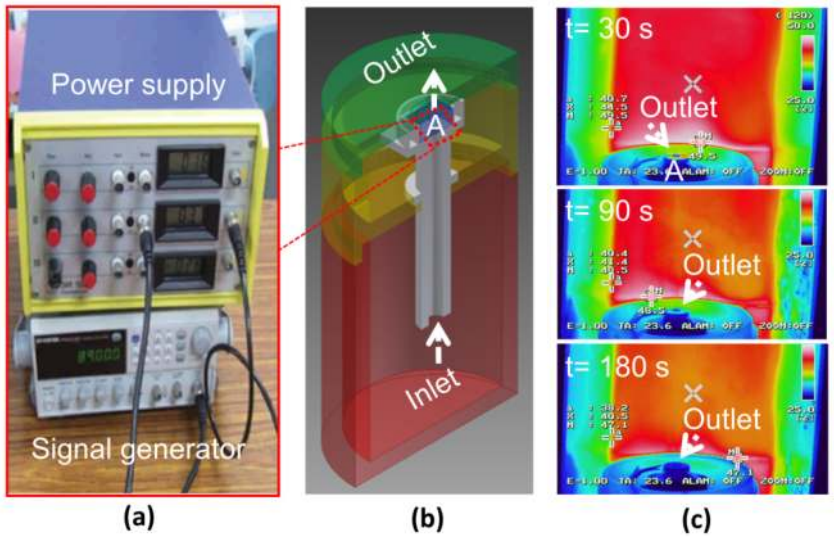

Figure 3. Integration, packaging, and test for a microsprayer: (a) electrical power supply and signal generator for controlling the micro-actuator during spraying, (b) liquid supply container integrated with the micro-actuator, and (c) thermography of droplet jetting with the electrical and liquid supply.

4. Characteristics of droplets in spray

From the view point of microfluidics, two significant respects can reflect the behaviour of a spray. One is the size and velocity of droplets, and the other is the rate and pattern of a spray. The former is primarily concerned with the kinematics of individual micro-droplets, while the latter is particularly emphasized to take into account the macrospraying phenomenon. Since either micro- or macro-behavior is important for a spray, one shall recognize their distinguishing characteristics entirely. Hence, the droplets in spray can be further elaborated and characterized as follows.

4.1. Size and velocity of a droplet

Conventionally, the size and velocity of a droplet can be visualized and calculated from particle image velocimetry (PIV), in which an expensive digital camera is used to perform the high-speed imaging capture (frame per second, *fps*, up to 10,000) for all droplets [29]. In this way, the droplet size distribution (DSD) and the others such as AMD and SMD can be calculated accordingly. From a practical view of convenience, while using a micro actuator mentioned previously, the initial velocity (v_0) of droplets on average can be simply evaluated as first-order approximation as proposed in Eq. (7), where η is the velocity coefficient, h_{nozzle} is the nozzle (via hole) thickness, and f_{drive} is the driving frequency, respectively. Moreover, assuming that the droplets travel a distance (s_a) under constant acceleration (a), this value (v_0) can be also correlated with the final average velocity (v_f) as expressed physically in Eq. (8):

$$v_0 = \eta \times (h_{nozzle} \times f_{drive}) \tag{7}$$

$$v_f^2 = v_0^2 + 2 \times a \times s_a \tag{8}$$

For instance, as demonstrated in Figure 4, a water spray was ejected from a piezoelectric micro-actuator at f_{drive} = 90 kHz, in which micro-nozzles featured an average thickness (h_{nozzle}) of 40 μm and an average diameter (d_{nozzle}) of 30 μm [37]. Using Eq. (7), the value of (v_0/η) was approximated as (30 μm)×(90×10^3/s) = 3.60 m/s. Thus, under normal gravity (i.e., a = 9.8 m/s^2) as demonstrated in Figure 4(a), this upward spray actually traveled a maximum distance s_a = 0.12 m to reach the final velocity v_f = 0. From Eq. (9) as ignoring the friction of air, the square of initial velocity was approximately calculated as 2×(9.8 m/s^2)×(0.12 m) = 2.35 m^2/s^2, yielding v_0 = 1.53 m/s and η = (1.53 m/s)/(3.60 m/s) = 0.425 (i.e., 42.5%); therefore, this high velocity hindered those droplets from being clearly imaged by normal optical cameras (fps = 30) as illustrated in Figure 4(b).

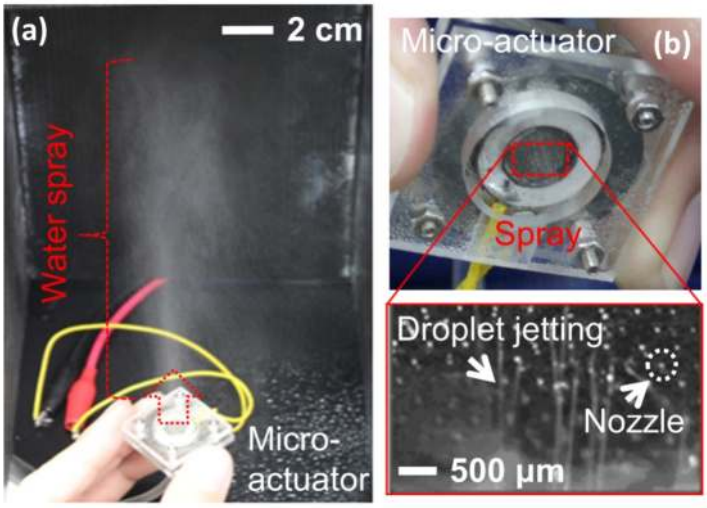

Figure 4. A group of droplets sprayed from a micro-actuator: (a) the upward formation of a water spray and (b) the downward droplet jetting from the micro-nozzles.

4.2. Rate and pattern of a spray

As a whole, the volumetric rate (ψ_r) of a microspray generated from the nozzles is straightforwardly determined by the droplet density (flux), driving frequency, and voltage. Again, using previous case as one example, the value of ψ_r for single droplet volume of 30 pl and firing nozzle number of 100 was estimated with a maximum of (30 pl)×100×(90×10^3 /s) = 0.27

ml/s = 16.20 ml/min. Nevertheless, this rate might drop dramatically due to failure of some nozzle during micro-actuation as shown in the inset of Figure 4(b). More importantly, the flow pattern of a spray was actually influenced by the flight velocity of droplets in air, typically leading to an appearance of turbulence [7,38]. In terms of fluid dynamics, this phenomenon pattern is associated particularly with a dimensionless Reynolds number (Re) as described in Eq. (9) [39]:

$$\mathrm{Re} = \frac{\rho \times v \times l}{\mu} \tag{9}$$

where ρ is the density of liquid, v is the droplet velocity, l is the characteristic length, and μ is the dynamic viscosity of liquid, respectively. For instance, Figure 5 shows PIV imaging for patterns of sprays generated from micro-nozzles (v = 3 m/s), in which the liquid of pure water exhibited the $\rho = 10^3$ kg/m^3 and $\mu = 10^{-3}$ Ns/m^2. Hence, the sparse spray (l < 1 mm) in Figure 5(a) was estimated with a low Re (< 3,000) such that it appeared like a laminar flow, while the turbulent flow with a large Re (> 15,000) was visualized for the dense spray (l < 5 mm) in Figure 5(b). Therefore, taking all of the characteristics of droplets into account, a variety of spray applications are described and illustrated in the next section.

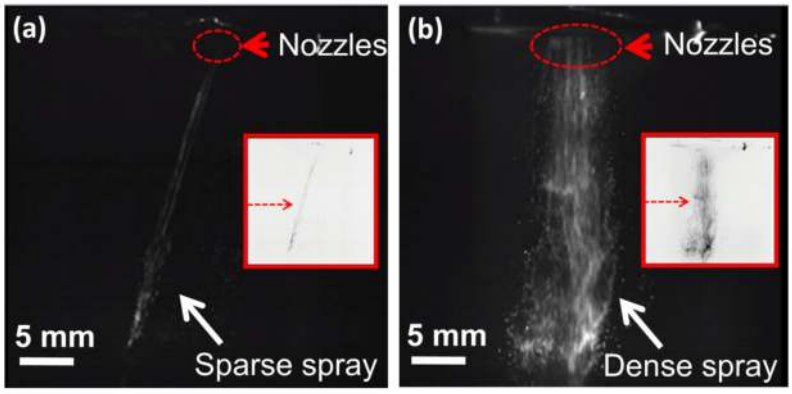

Figure 5. Various volume rates and microfluidic patterns of flow generated from the micro-nozzles of a micro-actuator: (a) a sparse spray and (b) a dense spray.

5. Applications

5.1. Droplet evaporative cooling

To date, droplet evaporative cooling (DEC) has been one of alternative means for reducing temperature of objects at low cost. It has been elaborated in decreasing the hot solid surfaces

with high values of CHF of 250–350 W/cm^2 [2,34]. Also, many other efforts have been made in the development of the spatial cooling systems, including the mechanical draft cooling tower and air-conditioning systems [28–29,40], in order to enhance the convective heat transfer in ambient environment. Figure 6(a) illustrates the photography pictures of such spray cooling circumstances, in which the conventional pumping liquid systems were operating indoors or outdoors. Also, using micro-actuators shown in Figure 6(b), the droplet ejection of water was periodically performed (between on and off) under ambient environment to demonstrate the temperature decrease of ~3°C visualized from the IR thermography [41].

(a)

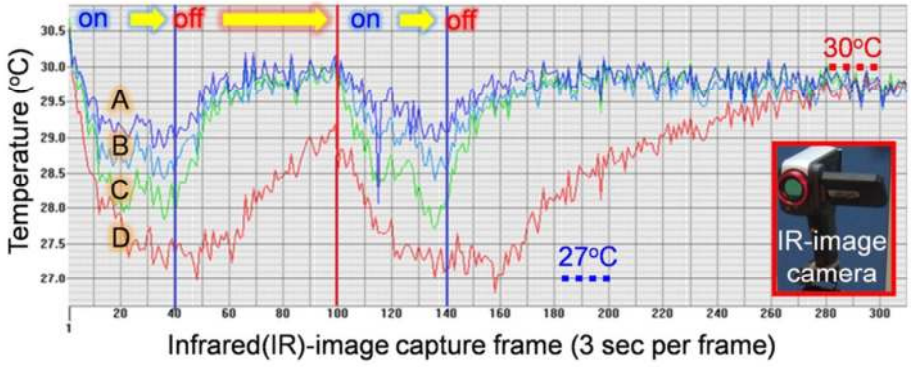

(b)

Figure 6. Evaporative cooling of droplets: (a) photography of water spray from traditional liquid supply outdoors and (b) temperature evolution of four positions (A, B, C, and D) over time within a spraying space, switching the micro-electronic actuator on (2 min) and off (3 min) alternatively during a period of 5 min.

In addition to the sprays of water, there are many colour liquids such as dye inks commercially available to be further adapted for industrial applications. Likewise, those inks have been used for direct and screen printing through generation of sprays as further discussed in the following.

http://dx.doi.org/10.5772/64756

5.2. Direct and screen printing

Instead of evaporating the liquid fully, ink deposition can be applied for printing as using diluted solutions with suitable solid content [42]. As a matter of fact, many printing methods have existed to date, mainly including the contact doctor-blade printing (DBP) method [43–46] and non-contact IJP method [8,33,47]. As compared to those DBP and IJP above, this kind of spray printing (SP) features the non-contact, high-speed, and large-area patterning capability [9,13]. With the assistance of one additional screen (mesh), the SP technique can be efficiently applied to perform the fine and complex patterning of micro-devices such as flexible dye-sensitized solar cells, polymer solar cell modules, and so forth [11,14].

For instance, Figure 7 demonstrates the spray printing of blue dye ink on a regular paper (A4 size) using a piezoelectric actuator and a mobile platform, in which direct printing of a spiral pattern (line width ~10 mm) and screen printing of a comb-type pattern (line width ~400 μm) were simply performed via a microelectronic controller (not shown here). Furthermore, fusing the novel materials from the emergence of nano-science and technology, those synthesized nanomaterials are suitable to be deposited and coated on substrates using the SP method for direct generation of thin functional films that is further described below.

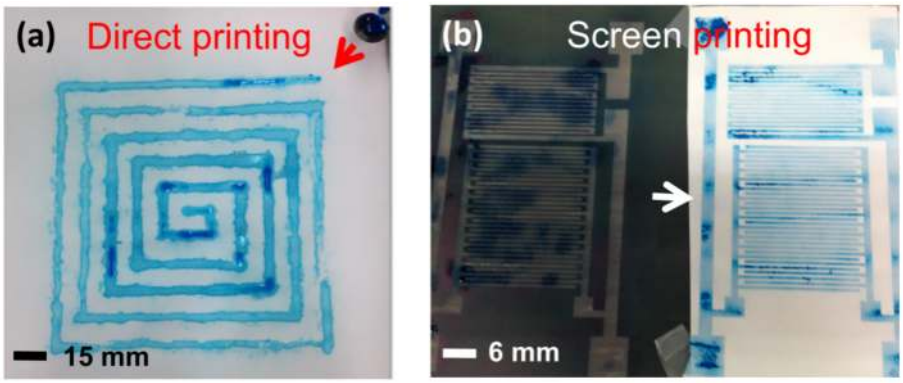

Figure 7. Spray printing of blue ink on a regular paper using a piezoelectric actuator: (a) direct printing of a square spiral pattern and (b) screen printing of a comb-type pattern.

5.3. Nanomaterial coating

The spray technique used as one of the deposition methods was thoroughly compared and analyzed with regard to solid oxide fuel cells (SOFC) applications by Will et al. [16], in which the formations of high-quality chemical composition films were emphasized. Besides those applications, a variety of nanomaterial coating with different chemical components were utilized in the study of spray printing (SP), which include nano-Cu particles and two-component Cu/Cu_2O [17], Cu and Ni particles [18], biomedical CaP ceramics [20], colloidal alumina particles [21], and silver (Ag) particles [22]. As shown in Figure 8, the silver ink diluted

with Ag nanoparticles was spray-printed on a flexible polyimide substrate, and then the dried film was formed after sintering. As can be seen clearly here in Figure 8(a), the grain-like boundaries were created due to insufficient adhesion of coating on substrate surface; the Ag particles typically less than 100 nm in size were also obtained as seen from the scanning electron microscope (SEM) picture in Figure 8(b). Poor electrical conductivity might be therefore expected in this case due to the non-uniformity of film morphology.

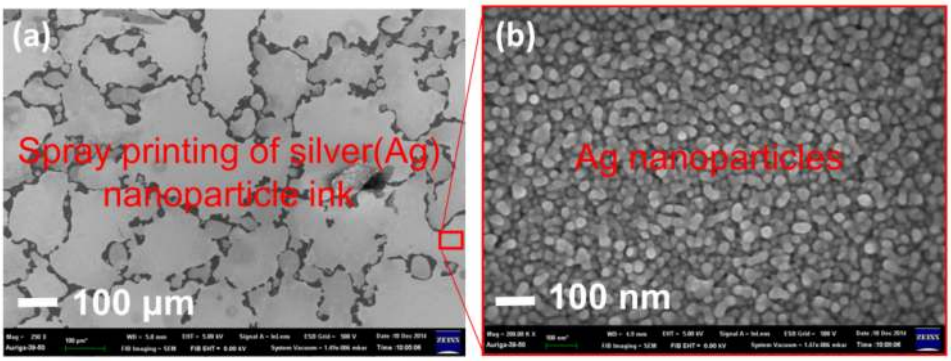

Figure 8. (a) Spray printing and sintering of silver (Ag) nanoparticle ink on polyimide surface and (b) magnified morphology of the printed Ag surface demonstrating the typical particle size less than 100 nm.

Obviously, it is noted here that the nanomaterial coating by spraying solutions may suffer from the weak interfacial strength between two layers of different materials. Nevertheless, compared to conventional deposition techniques such as PVD and CVD, this material coating application no doubt benefits low cost and time for processing, and therefore the interfacial problem deserves to be further improved in the future.

5.4. Liquid nebulization

For years, liquid nebulization has been generally used as an effective treatment for human airway disease such as panting. Mostly, with synthesis of different component concentrations and functions, aerosol delivery of pulmonary drug to human lungs is performed through spraying for medical therapy [48–49]. Because of the breathing need for patient therapy, those drug droplets of a spray generated from medical nebulizers typically feature an extremely small size (< 5 μm) to yield a high efficient absorption, in which the delivered amount of active drug could be as low as 20 mg for 4 h. Furthermore, micro actuators integrated with micron-sized nozzles are commonly applied in the nebulizers that have been commercialized and marketed over 10 years. As demonstrated in Figure 9, the portable and hand-held nebulizers with a compact size (e.g., 6.3 cm×6.4 cm×15 cm for NH60) are available for quietly generating aerosol of different drugs such as albuterol, ipratropium, sulfate, etc. Aerosol performance on nebulization rate can be adjusted and controlled by users.

Figure 9. (a) Packet Air™ portable nebulizer by Microbase Inc. and (b) handheld tubeless nebulizer NH60 by Rossmax International Ltd.

5.5. Miscellaneous

In fact, all applications of the spray science and technology are quite versatile in many respects beyond those mentioned earlier [50–52]. The new development and progress in spray science and techniques can continue to be applied to more novel compound materials and microstructured devices such as those demonstrated in the solar and fuel cells. Yet, the other multidisciplines and creative ideas are being further blended into the field of sprays, perhaps yielding more fruitful applications in the future.

6. Concluding remarks

Over decades, many studies of science and technology have demonstrated the sprays to serve as an effective and efficient means for generation and evaporation of droplets. Many fundamental factors considered for pursuing the high-quality spraying involve appropriate selections of working liquids, operating actuators, droplet generation and evaporation, and spraying control. Preliminary design issues of microsprays concerning micro-actuators, nozzles, system integration, and control can be overcome by understanding and realizing fundamentals of working principles. Many applications in daily life and industry that include droplet evaporative cooling (DEC), direct and screen printing (SP), nanomaterial coating (NMC), and liquid nebulization (LN) have been demonstrated using spray techniques. In the future, this knowledge of science and technologies blended with the emergence of novel materials and devices may be promoted to the next generation of sprayers with higher performance than ever.

Acknowledgements

The author thanks research grant for this work partially by the Ministry of Science and Technology (MOST) under MOST 104-2221-E-151-036-MY2, Taiwan, ROC.

Author details

Chin-Tai Chen*

Address all correspondence to: chintai@kuas.edu.tw

Department of Mechanical Engineering, National Kaohsiung University of Applied Sciences, Kaohsiung, Taiwan, ROC

References

[1] Andreas E. Time constants for the evolution of sea spray droplets. Tellus. 1990; 42B: 481-497.

[2] Marcos A, Chow L, Du JH, Lei S. Spray cooling at low system pressure. In: Proceedings of 18th IEEE SEMI-THERM Symposium; 2002. p. 169-175.

[3] Yang JC, Chien W, King M,Grosshandler WL. A simple piezoelectric droplet generator.Exp. Fluids. 1997; 23: 445-447.

[4] Demirci U, Goksenin G, Yaralioglu G, Haggstrom E, Khuri-Yakub, BT. Femtoliter to picoliter droplet generation for organic polymer deposition using single reservoir ejector arrays. IEEE Trans. Semicond. Manuf. 2005;18: 709-714.

[5] Sommerfeld M, Qiu, HH. Experimental studies of spray evaporation in turbulent flow. Int. J. Heat. Fluid. Flow. 1998; 19: 10-22.

[6] Fisenko SP, Wang WN, Lenggoro IW, Okyuama K. Evaporative cooling of micron-sized droplets in a low-pressure aerosol reactor. Chem. Eng. Sci. 2004; 61: 6029-6034.

[7] Li T, Nishida K, Hiroyasu H. Droplet size distribution and evaporation characteristics of fuel spray by a swirl type atomizer. Fuel. 2011; 90: 2367-2376.

[8] Hart AL, Turner APF, Hopcroft D. On the use of screen- and ink-jet printing to produce amperometric enzyme electrodes for lactate. Biosens. Bioelectron.1996; 11: 263-270.

[9] Jang Y, Park YD, Lim JA, Lee HS, Lee WH, Cho K. Patterning the organic electrodes of all-organic thin film transistors with a simple spray printing technique. Appl. Phys. Lett. 2006; 89: 183501.

[10] Dong TY, Chen WT, Wang CW, Chen CP, Chen CN, Lin MC, Song JM, Chen IG, KaoTH. One-step synthesis of uniform silver nanoparticles capped by saturated decanoate: direct spray printing ink to form metallic silver films. Phys. Chem. Chem. Phys. 2009; 11: 6269-6275.

[11] Peng Y, Zhong J, Wang K, Xue B, Cheng YB. A printable graphene enhanced composite counter electrode for flexible dye-sensitized solar cells. Nano Energy. 2013; 2: 235-240.

[12] Abdelhalim A, Abdellah A, Scarpa G, Lugli P. Fabrication of carbon nanotube thin films on flexible substrates by spray deposition and transfer printing. Carbon. 2013; 61: 72-79.

[13] Klim D, Baeg KJ, Yu BK, Kang SJ, Kang M, Chen Z, Facchetti A, Kim DY, Noh YY. Spray-printed organic field-effect transistors and complementary inverters. J. Mater. Chem. C. 2013; 1: 1500-1506.

[14] Back H, Kong J, Kang H, Kim J, Kim JR, Lee K. Flexible polymer solar cell modules with patterned vanadium suboxide layers deposited by an electro-spray printing method. Sol. Energy Mater. Sol. Cells. 2014; 130: 555-560.

[15] Chen CT. Inkjet printing of microcomponents: theory, design, characteristics and applications. In: Kamanina N. (editor). Features of Liquid Crystal Display Materials and Processes. Croatia: InTech; 2011. p.43-60. DOI: 10.5722/26225.

[16] Will J,Mitterdorfer A, Kleinlogel D, Perednis D, Gauckler LJ. Fabrication of thin electrolytes for second-generation solid oxide fuel cells. Solid State Ionics. 2000; 131: 79-96.

[17] Schulz DL, Curtis CJ, Ginley DS. Surface chemistry of copper nanoparticles and direct spray printing of hybrid particle/metallorganic inks.Electrochem. Solid State Lett. 2001; 4: C58-C61.

[18] Kim JH, Babushok VI, Germer TA, Mulholland GW, Ehrman SH. Co-solvent assisted spray pyrolysis for the generation of metal particles. J. Mater. Res. 2003; 18: 1611-1622.

[19] Makela JM, Keskinen H, Foesblom T, Keskinen J. Generation of metal and metal oxide nanoparticles by liquid flame spray process. J. Mater. Sci. 2004; 39: 2783-2788.

[20] Leeuwenburgh SCG, Wolke JGC, Schoonman J, Jansen JA. Influence of deposition parameters on morphological properties of biomedical calcium phosphate coatings prepared using electrostatic spray deposition. Thin Solid Films. 2005; 472: 105-113.

[21] Sen D, Mazumder S, Melo JS, Khan A, Bhattyacharya S, D'Souza SF. Evaporation driven self-assembly of a colloidal dispersion during spray drying: volume fraction dependent morphological transition. Langmuir. 2009; 25: 6690-6695.

[22] Park M, Im J, Shin M, Min Y,Park J, Cho H, Park S, Shim MB, Jeon S, Chung DY, Bae J, Park J, Jeong U, Kim K. Highly stretchable electric circuits from a composite material of silver nanoparticles and elastomeric fibres, Nat. Nanotechnol. 2012; 7: 803-809.

[23] McPeck M, Tandon R, Hughes K, Smaldone GC. Aerosol delivery during continuous nebulization. Chest. 1997; 111: 1200-1205.

[24] Wiedmann TS, DeCastro L, Wood RW. Nebulization of nanocrystals: production of a respirable solid-in-liquid-in-air colloidal dispersion. Pharm. Res. 1997; 14: 112-116.

[25] Hertel SP, Winter G, Friess W. Protein stability in pulmonary drug delivery via nebulization. Adv. Drug Deliv. Rev. 2015; 93: 79-94.

[26] Erbil HY. Evaporation of pure liquid sessile and spherical suspended drops: a review. Adv. Colloid Interface Sci. 2012; 170: 67-86.

[27] Kang D, Strand RK. Modeling of simultaneous heat and mass transfer within passive down-draft evaporative cooling (PDEC) towers with spray in FLUENT. Energy Build. 2013; 62: 196-209.

[28] Koseoglu MF. Investigation of water droplet carryover phenomena in industrial evaporative air-conditioning systems. Int. Commun. Heat Mass Transf. 2013; 47: 92-97.

[29] Montazeri H, Blocken B, Hensen JLM. Evaporative cooling by water spray systems: CFD simulation, experimental validation and sensitivity analysis. Build. Environ. 2015; 83: 129-141.

[30] Chen CT, Wang HY. Droplet generation and evaporative cooling using micro piezoelectric actuators with ring-surrounded circular nozzles. Microsyst. Technol. 2015; 21: 2067-2075.

[31] Rahman K, Ko JB, Khan S, Kim DS, Choi KH. Simulation of droplet generation through electrostatic forces. J. Mech. Sci. Technol. 2010; 24: 307-310.

[32] Li R, Ashgriz N, Chandra S. Droplet generation from pulsed micro-jets. Exp. Therm. Fluid Sci. 2008; 32: 1679-1686.

[33] Hu BC, Weng RH, Chen CT. Silver conducting lines of dye-sensitized solar cells printed onto commercial building tiles. Proc. Eng. 2014: 79: 267-272.

[34] Sawyer ML, Jeter SM, Abdel-Khalik SI. A critical heat flux correlation for droplet impact cooling. Int. J. Heat Mass Transf. 1997; 40: 2123-2131.

[35] Mugele RA, Evans HD. Droplet size distribution in sprays. Ind. Eng. Chem. 1951; 43: 1317-1324.

[36] Semiao V, Andrade P, da GracaCarvalho M. Spray characterization: numerical prediction of Sauter mean diameter and droplet size distribution. Fuel. 1996; 75: 1707-1714.

[37] Huang JJ, Chen CT. Microelectroforming of a nickel nozzle plate featured with antistiction for a piezoelectric atomizer. In: Proceedings of IEEE-NEMS. 2013;p.490-493.

[38] Kah D, Laurent F, Massot M, Jay S. A high order moment method simulating evaporation and advection of a polydisperse liquid spray. J. Comput. Phys. 2012; 231: 394-422.

[39] Miyatake O, Koito Y, Tagawa K, MarutaY. Transient characteristics and performance of a novel desalination system based on heat storage and spray flashing. Desalination. 2001; 137: 157-166.

[40] Fisenko SP, Brin AA, Petruchik AI. Evaporative cooling of water in a mechanical draft cooling tower. Int. J. Heat Mass Transf. 2004; 47: 165-177.

[41] Wang HY, Huang C, Chen C. T. Specific design and implementation of a piezoelectric droplet actuator for evaporative cooling of free space. In: Proceedings of IEEE-NEMS. 2012;p.419-422.

[42] Nagata R, Yokoyama K, Clark SA, Karube I. A glucose sensor fabricated by the screen printing technique. Biosens. Bioelectron. 1995; 10: 261-267.

[43] Shaheen SE, Radspinner R, Peyghambarian N, Jabbour GE. Fabrication of bulk heterojunction plastic solar cells by screen printing. Appl. Phys. Lett. 2001; 79: 2996-2998.

[44] Krebs FC, Alstrup J, Spanggaard H, Larsen K, Kold E. Production of large-area polymer solar cells by industrial silk screen printing, lifetime considerations and lamination with polyethyleneterephthalate. Sol. Energy Mater. Sol. Cells. 2004; 123: 749-756.

[45] Krebs FC, Jorgensen M, Norrman K, Hagemann O, Alstrup J, Nielsen TD, Fyenbo J, Larsen K, Kristensen J. A complete process for production of flexible large area polymer solar cells entirely using screen printing. Sol. Energy Mater. Sol. Cells. 2009; 93: 422-441.

[46] Krebs FC. Polymer solar cell modules prepared using roll-to-roll methods: knife-over-edge coating, slot-die coating and screen printing. Sol. Energy Mater. Sol. Cells. 2009; 93: 465-475.

[47] Wang MW, Pang DC, Tseng YE, Tseng CC. The study of light guide plate fabricated by inkjet printing technique. J. Taiwan Inst. Chem. Eng. 2014; 45: 1049-1055.

[48] McPeck M, Tandon R, Hughes K, Smaldone GC. Aerosol delivery during continuous nebulization. Chest. 1997; 111: 1200-1205.

[49] Hertel SP, Winter G, FriessW. Protein stability in pulmonary drug delivery via nebulization. Adv. Drug Deliv. Rev. 2014; DOI: 10.1016/j.addr.2014.10.003.

[50] Sazhin SS, Martynov SB, Kristyadi T, Crua C, Heikal MR. Diesel fuel spray penetration, heating, evaporation and ignition: modelling vs. experimentation. Int. J. Eng. Syst. Model. Simul. 2008;1: 1-19.

[51] Li T, Nishida K, Hiroyasu H. Droplet size distribution and evaporation characteristics of fuel spray by a swirl type atomizer. Fuel. 2011; 90: 2367-2376.

[52] Tveen-Jensen K, Gesellchen F, Wilson R, Spickett CM, Cooper JM, Pitt PR. Interfacing low-energy SAW nebulization with liquid chromatography-mass spectrometry for the analysis of biological samples. Sci. Rep. 2015; 5: 9736.